Received: 7 February 2022 | Revised: 13 June 2022 | Accepted: 13 July 2022

DOI: 10.1002/alz.12763

Alzheimer's & Dementia®
THE JOURNAL OF THE ALZHEIMER'S ASSOCIATION

FEATURED ARTICLE

Differential diagnosis of amnestic dementia patients based on an FDG-PET signature of autopsy-confirmed LATE-NC

Michel J. Grothe[1,2,3] | **Alexis Moscoso**[3] | **Jesús Silva-Rodríguez**[1] | **Catharina Lange**[4] | **Kwangsik Nho**[5] | **Andrew J. Saykin**[5] | **Peter T. Nelson**[6] | **Michael Schöll**[3,7] | **Ralph Buchert**[8] | **Stefan Teipel**[2,9] | **for the Alzheimer's Disease Neuroimaging Initiative***

[1]Unidad de Trastornos del Movimiento, Servicio de Neurología y Neurofisiología Clínica, Instituto de Biomedicina de Sevilla, Hospital Universitario Virgen del Rocío/CSIC/Universidad de Sevilla, Seville, Spain

[2]German Center for Neurodegenerative Diseases (DZNE), Rostock, Germany

[3]Wallenberg Center for Molecular and Translational Medicine and Department of Psychiatry and Neurochemistry, University of Gothenburg, Gothenburg, Sweden

[4]Charité – Universitätsmedizin Berlin, corporate member of Freie Universität Berlin and Humboldt-Universität zu Berlin, Department of Nuclear Medicine, Berlin, Germany

[5]Indiana Alzheimer's Disease Research Center and Department of Radiology and Imaging Sciences, Indiana University School of Medicine, Indianapolis, Indiana, USA

[6]Sanders-Brown Center on Aging and Department of Pathology, University of Kentucky, Lexington, Kentucky, USA

[7]Department of Neurodegenerative Disease, UCL Institute of Neurology, London, UK

[8]Department of Diagnostic and Interventional Radiology and Nuclear Medicine, University Medical Center Hamburg-Eppendorf, Hamburg, Germany

[9]Department of Psychosomatic Medicine, Rostock University Medical Center, Rostock, Germany

Correspondence
Michel J. Grothe, Unidad de Trastornos del Movimiento, Servicio de Neurología y Neurofisiología Clínica, Instituto de Biomedicina de Sevilla, Hospital Universitario Virgen del Rocío/CSIC/Universidad de Sevilla, Avda. Manuel Siurot s/n, 41013 Seville, Spain.
Email: mgrothe@us.es

*Data used in preparation of this article were obtained from the Alzheimer's Disease Neuroimaging Initiative (ADNI) database (http://adni.loni.usc.edu/). As such, the investigators within the ADNI contributed to the design and implementation of ADNI and/or provided data but did not participate in analysis or writing of this report. A complete listing of ADNI investigators can be found at: http://adni.loni.usc.edu/wp-content/uploads/how_to_apply/ADNI_Acknowledgement_List.pdf

Funding information
Instituto de Salud Carlos III; Fondo Europeo de Desarrollo Regional; NIH, Grant/Award

Abstract

Introduction: Limbic age-related TDP-43 encephalopathy neuropathologic change (LATE-NC) is common in advanced age and can underlie a clinical presentation mimicking Alzheimer's disease (AD). We studied whether an autopsy-derived fluorodeoxyglucose positron emission tomography (FDG-PET) signature of LATE-NC provides clinical utility for differential diagnosis of amnestic dementia patients.

Methods: *Ante mortem* FDG-PET patterns from autopsy-confirmed LATE-NC ($N = 7$) and AD ($N = 23$) patients were used to stratify an independent cohort of clinically diagnosed AD dementia patients ($N = 242$) based on individual FDG-PET profiles.

Results: Autopsy-confirmed LATE-NC and AD groups showed markedly distinct temporo-limbic and temporo-parietal FDG-PET patterns, respectively. Clinically diagnosed AD dementia patients showing a LATE-NC–like FDG-PET pattern ($N = 25$, 10%) were significantly older, showed less abnormal AD biomarker levels, lower *APOE* ε4, and higher *TMEM106B* risk allele load. Clinically, they exhibited a more memory-predominant profile and a generally slower disease course.

Numbers: R01 LM013463, P30 AG010133, P30 AG072976, R01 AG019771, R01 AG057739, U01 AG024904, R01 LM013463, R01 AG068193, T32 AG071444, U01 AG068057, U01 AG072177, R01 AG057187, P30 AG072946, RF1 NS118584; Alice Wallenberg Foundation (Wallenberg Centre for Molecular and Translational Medicine), Grant/Award Number: KAW 2014.0363; Swedish Research Council, Grant/Award Number: #2017-02869; Swedish state under the agreement between the Swedish government and the County Councils, Grant/Award Number: #ALFGBG-813971; Swedish Alzheimer Foundation, Grant/Award Number: #AF-740191

Discussion: An autopsy-derived temporo-limbic FDG-PET signature identifies older amnestic patients whose clinical, genetic, and molecular biomarker features are consistent with underlying LATE-NC.

KEYWORDS
amyloid, apolipoprotein E, autopsy, fluorodeoxyglucose positron emission tomography, hippocampal sclerosis, limbic age-related TDP-43 encephalopathy, tau, TDP-43, TMEM106B

1 | INTRODUCTION

Although Alzheimer's disease (AD) is the most common neurodegenerative pathology underlying dementia in the elderly, several other age-related pathologies may result in similar memory-predominant dementia syndromes, and large-scale autopsy series have estimated that approximately 15% to 30% of clinically diagnosed AD dementia patients do not meet neuropathologic criteria for AD.[1,2] One of the most common neurodegenerative pathologies that may mimic AD clinically in older patients is limbic TDP-43 proteinopathy, which has recently been categorized as a distinct disease entity called limbic-predominant age-related TDP-43 encephalopathy (LATE).[3] LATE neuropathologic change (LATE-NC) is particularly frequent at advanced age and is often accompanied by severe hippocampal degeneration disproportionate to the amount of tangle pathology (i.e., hippocampal sclerosis [HS]), as well as with amnestic deficits that are indistinguishable from those caused by AD in standard clinical evaluations.[3,4] While the condition is most often comorbid with AD pathology,[5,6] a significant portion of clinically diagnosed AD dementia patients are found to have LATE-NC without fulfilling neuropathologic criteria for AD, indicating that LATE-NC is the main pathologic driver of the amnestic deficits in these cases.[7–10]

Pathologic association studies have revealed some characteristic clinical and genetic features of LATE-NC in the absence of significant AD pathology, including a more memory-predominant neuropsychological profile with relative sparing of executive functions and a generally more protracted course of global cognitive decline compared to AD.[3,11] In contrast to AD, LATE-NC also associates with the *TMEM106B* and *GRN* risk alleles previously linked to TDP-43 pathology in frontotemporal lobar degeneration.[12–14] The apolipoprotein E (*APOE*) ε4 allele was also found to be associated with LATE-NC, although to a lesser degree compared to AD.[15,16]

To date, no validated molecular imaging or fluid biomarker specific for TDP-43 pathology exists that would allow detecting LATE-NC during lifetime.[3] However, recent neuroimaging–pathologic correlation studies could provide evidence that limbic TDP-43 pathology associates with specific neurodegenerative features that could be used as indirect neuroimaging biomarkers to detect the condition in vivo.[17–21] Particularly, a recent *ante mortem* fluorodeoxyglucose positron emission tomography (FDG-PET) imaging study found that amnestic patients with limbic TDP-43 pathology and HS were characterized by a specific temporolimbic-predominant neurodegeneration pattern that distinguished them from autopsy-confirmed AD cases without comorbid TDP-43.[21]

Here, we reassessed the LATE-NC–associated FDG-PET pattern in an independent autopsy cohort, and then further studied the clinical utility of this pattern as a topographic imaging biomarker for in vivo stratification of a larger sample of clinically diagnosed AD dementia patients.

2 | METHODS

2.1 | Study participants

Participants included in this study were enrolled in the Alzheimer's Disease Neuroimaging Initiative (ADNI) cohort. For the identification of LATE-NC- and AD-typical FDG-PET patterns, we examined data from the subsample of ADNI participants who had been followed to autopsy and who had standardized data from neuropathological examinations. In this "autopsy cohort" (data freeze: 17/05/2021), we identified a total of 58 participants who had a clinical diagnosis of AD dementia (N = 50) or amnestic mild cognitive impairment (MCI; *N* = 8) at last clinical evaluation and available *ante mortem* FDG-PET scans. These participants were further classified according to their neuropathological characteristics (see the Neuropathological Assessments section). We restricted our analyses to participants with cognitive impairment because early, clinically silent pathology may have only subtle, or even reverse, effects on the FDG-PET signal[22] (see Figure S1 in supporting information for a flowchart of patient selection). The average interval between last clinical evaluation and death was 1.9 ± 1.7 years, and between last available FDG-PET acquisition and death 3.3 ± 2.3 years.

To study the utility of the autopsy-derived FDG-PET patterns for in vivo patient stratification, we analyzed data from a separate "in vivo cohort" of 242 clinically diagnosed AD dementia patients, corresponding to all ADNI participants with a baseline diagnosis of AD dementia

and availability of an FDG-PET scan (query date: 10/07/2018), who were not included in the autopsy sample used to define the pathology-specific FDG-PET patterns. The average interval between FDG-PET scanning and clinical assessment was 9 ± 18 days.

For reference, we included normative FDG-PET data of a group of 179 healthy controls in ADNI that was also used in our previous FDG-PET analyses.[23] This group had Mini-Mental State Examination (MMSE) scores between 26 and 30 (average: 29.1 ± 1.2), ranged in age from 60 to 90 years (average: 73.8 ± 6.5), and had equal sex distribution (50% female).

All participants provided written informed consent and data collection and sharing were approved by the institutional review board of each institution participating in ADNI.

2.2 | Neuropathological assessments

Neuropathological assessments were performed by the ADNI Neuropathology Core, which provides standardized neuropathologic assessments of autopsied ADNI participants (http://adni.loni.usc.edu/about/#core-container).[24] According to National Institute on Aging–Alzheimer's Association guidelines,[25] evidence of AD neuropathologic change (ADNC) is classified as absent, low, intermediate, or high based on combined information from Thal amyloid beta (Aβ) phases, Braak neurofibrillary tau tangle staging, and Consortium to Establish a Registry for Alzheimer's Disease (CERAD) score for density of neuritic plaques. Assessment of TDP-43 pathology follows a standardized regional evaluation of TDP-43-immunoreactive inclusions in the spinal cord, amygdala, hippocampus, entorhinal cortex/inferior temporal gyrus, and frontal neocortex.[26] In the present study, presence of limbic TDP-43 pathology was defined based on TDP-43-immunoreactive inclusions in any of the following regions: amygdala, hippocampus, and/or entorhinal cortex/inferior temporal gyrus.

A total of 27 autopsy cases had evidence of limbic TDP-43 pathology indicative of LATE-NC, including 7 cases without comorbid AD (i.e., absent or low ADNC; "pure LATE-NC"), and 20 cases who also had intermediate to high ADNC ("AD+LATE-NC"). In addition, 23 cases had relatively pure AD pathology without comorbid TDP-43 pathology. Three of the pure LATE-NC cases (43%), two of the AD+LATE-NC cases (10%), and none of the pure AD cases had pathologically confirmed HS.

2.3 | Determination of pathology-specific FDG-PET patterns

All FDG-PET scans used in this study were downloaded from the ADNI server in fully pre-processed format (see http://adni.loni.usc.edu/methods/documents/ for details) and then spatially normalized to a customized FDG-PET template in Montreal Neurological Institute (MNI) standard space using SPM8.[27] We estimated LATE-NC-typical and AD-typical FDG-PET patterns by contrasting FDG-PET data of the pure LATE-NC and AD groups against normative data from healthy controls using voxel-wise 2-sample *t*-tests in SPM.[23] To better understand the effect of comorbid pathology on the FDG-PET pattern, we also studied the FDG-PET pattern of the AD+LATE-NC group compared to healthy controls as well as compared to the pure AD group. FDG-PET images were scaled to a pons reference region (manually drawn in MNI space), smoothed with an 8mm isotropic kernel, and regions with less than 50% gray matter probability in the segmented MNI152 template were excluded.[23,28] Statistical parametric maps of the group differences were expressed as Cohen's d effect size maps to reveal the brain-wide hypometabolic patterns (using the formula $d = t * \sqrt{\frac{1}{n1} + \frac{1}{n2}}$).[29]

We further conducted region-of-interest (ROI) analyses of medial temporal (amygdala and hippocampus) and inferior temporal ROIs, which were defined using the Harvard-Oxford anatomical atlas (with 25% probability threshold). These ROIs had previously been found to constitute prominent features of the LATE-NC/HS-associated FDG-PET pattern, and the inferior-to-medial temporal metabolism (IMT) ratio was proposed as a simplified biomarker metric to capture this pattern.[20,21] ROI values were extracted from unsmoothed pons-scaled FDG-PET images and differences were compared between groups using *t*-tests. The IMT ratio was further used in a receiver operating characteristic (ROC) curve analysis to assess its accuracy for pathologic group separation.[20]

RESEARCH IN CONTEXT

1. **Systematic Review**: We reviewed the literature using standard search engines (e.g., PubMed and Google Scholar). While some previous studies have examined relationships of limbic-predominant age-related TDP-43 encephalopathy neuropathologic change (LATE-NC) and/or hippocampal sclerosis with specific neuroimaging features, these have mainly focused on magnetic resonance imaging scans and assessments of medial temporal lobe structure. Only two recent studies have examined associations with fluorodeoxyglucose positron emission tomography (FDG-PET), and none of the existing studies have assessed the clinical utility of the associated neuroimaging features for in-vivo patient stratification.
2. **Interpretation**: Our findings corroborate that LATE-NC associates with a distinct temporo-limbic FDG-PET pattern. We demonstrate the clinical utility of this pattern for differential diagnosis of amnestic dementia by showing that clinically diagnosed Alzheimer's disease (AD) dementia patients exhibiting this pattern had lower AD biomarker levels and showed distinct clinical and genetic features consistent with LATE-NC.
3. **Future Directions**: Future studies should aim to identify patients with a LATE-NC FDG-PET pattern at earlier, pre-dementia disease stages and study their future clinical evolution.

2.4 | Classification of individual FDG-PET patterns in the in vivo cohort

We assessed the correspondence between an individual patient's hypometabolic pattern and the LATE-NC-typical and AD-typical patterns using an automated pattern matching approach based on spatial correlation.[28,30] First, for each patient in the in vivo cohort we calculated the individual's hypometabolic profile based on regional z-scores (referenced to the healthy control data) across all 52 cortical and subcortical gray matter regions defined in the Harvard-Oxford atlas. For individuals with hypometabolism (defined as $z \leq -1.5$) in any of the relevant brain areas associated with AD or LATE-NC (Table S1 in supporting information), we then assessed the spatial correlation between the individual's regional z-scores and the respective regional effect size scores of the pathology-specific patterns (note that for robustness we chose to use ROI-wise instead of voxel-wise spatial correlations).[28,30,31] Patients showing a statistically significant correlation (i.e., $r > 0.28$, $P < 0.05$) with any of the two patterns were then ordered along a continuum from most AD-like to most LATE-NC-like hypometabolism, quantified by the delta score between the respective spatial correlation coefficients ($\Delta r = r[AD] - r[LATE\text{-}NC]$; see Figure S2 in supporting information). Finally, aiming to maximize the difference in patterns between the stratified groups we applied a cutoff of $|\Delta r| > 0.28$ to classify the upper and lower parts of the Δr spectrum as clearly "LATE-NC-like" and clearly "AD-like." While naturally arbitrary, this $|\Delta r| > 0.28$ cutoff ensures that the same topographic threshold is used for the AD-like and LATE-NC-like pattern classifications. In complementary analyses we also explored an alternative Gaussian mixture model approach for patient stratification (Figure S3, Table S2 in supporting information), and further studied the Δr value as a continuous variable.

In addition, we also stratified the patients according to the previously proposed IMT ratio,[21] using the cutoff that provided best group separation between the pathologically defined groups in the autopsy cohort.

2.5 | Neuropsychological evaluation

We used MMSE scores for characterizing global cognitive impairment, as well as previously established composite cognitive scores for assessing memory (ADNI-MEM) and executive function (ADNI-EF) impairment (see supporting information).[32,33] In addition, we calculated a "cognitive profile" variable as the difference between the ADNI-MEM and the ADNI-EF composite scores (ΔMEM-EXEC) to characterize relative impairments in these two domains.[23] In addition to baseline assessments, 223 patients (92%) had at least one follow-up cognitive assessment, and the average follow-up time was 1.5 ± 0.9 years.

2.6 | Molecular biomarkers and genetics

A subset of 175 patients (72%) in the in vivo cohort had complete cerebrospinal fluid (CSF) biomarker data available. In the present study, we included peptide levels of $A\beta_{1\text{-}42}$ and tau phosphorylated at threonine 181 (p-tau181) measured using the fully automated Roche Elecsys electrochemiluminescence immunoassays as described previously.[34]

APOE genotype was determined by Cogenics using standard methods to genotype the two *APOE* ε4-defining single nucleotide polymorphisms (SNPs; rs429358, rs7412).[35] This information was available for all but one individual in the in vivo cohort. Genotyping of the *GRN* (rs5848) and *TMEM106B* risk SNPs (rs1990622) was performed using Illumina genome-wide association study genotyping assays as described in detail previously.[35,36] Quality-controlled genotyping results for the rs5848 and rs1990622 SNPs were available for 87% (210/242) of the study sample.

2.7 | Statistical analysis

Demographic, clinical, and biomarker characteristics were compared between the stratified patient groups using two-sample *t*-tests, Mann-Whitney U tests, or Fisher's exact tests depending on the assessed variable. Differences in cognitive trajectories between LATE-NC-like and AD-like patient groups were assessed using linear mixed effects models, which included participant-specific intercepts and slopes. Group differences in *APOE* ε4, *TMEM106B* "T," and *GRN* "T" risk alleles were analyzed under additive models using logistic regression. Associations with LATE-NC-like versus AD-like pattern expression on a continuous scale were assessed using Pearson's correlation analysis with the Δr score. Statistical analyses were carried out using IBM SPSS Statistics (version 21) and Matlab; the significance threshold was set at $P < 0.05$. We did not apply a correction for multiple comparisons in this hypothesis-driven study with a limited number of planned comparisons.[37]

3 | RESULTS

3.1 | Pathology-specific FDG-PET patterns

Demographics and neuropathological details for the pathology-defined groups are shown in Table 1. Compared to healthy controls, the AD group showed the well-described pattern of AD-typical hypometabolism that is most pronounced in temporo-parietal areas, while also affecting the medial temporal lobe (Figure 1A). Interestingly, the hypometabolic pattern of the AD+LATE-NC group was highly similar to the AD group (Figure 1B). By contrast, the LATE-NC group showed a strikingly different pattern characterized by a much more pronounced involvement of the medial temporal lobe and related limbic areas, and less pronounced involvement of inferior temporal and parietal areas (Figure 1C). Highest effect sizes ($d = 0.5$ to 1) of group differences between LATE-NC and AD were observed in the medial temporal lobe and insula/fronto-opercular cortex (LATE-NC<AD), as well as in inferior temporal and lateral parietal areas (AD<LATE-NC; Figure 1D).

ROI analysis confirmed that medial temporal FDG-PET signal was lower in LATE-NC compared to AD ($d = 0.90$, $P = 0.046$), whereas

TABLE 1 Autopsy cohort

	LATE-NC w/o AD	AD w/o LATE-NC	AD + LATE-NC
N	7	23	20
Age at death (years)	87.6 ± 5.6	80.4 ± 8.2	82.5 ± 8.1
Sex (M/F)	5/2	15/8	14/6
aMCI/ADD	3/4	1/22	1/19
Interval diagnosis to death	1.6 ± 1.6	1.7 ± 1.4	2.6 ± 2.2
Interval FDG-PET to death	3.6 ± 3.5	3.1 ± 2.3	3.8 ± 2.4
A, 0/1/2/3	0/3/4/0	0/0/1/22	0/0/0/20
B, 0/1/2/3	0/6/1/0	0/0/1/22	0/0/1/19
C, 0/1/2/3	4/3/0/0	1/0/2/20	0/1/1/18
TDP-43 stage, 1/2/3	0/5/2	N/A	2/13/5
Lewy body pathology, 0/1/2/3/4, %pos	3/1/0/3/0, 57%	12/1/0/5/5, 48%	7/0/1/7/5, 65%
FTD-related TDP-43 (FTDTDP)	0/7, 0%	0/23, 0%	1/20, 5%
Argyrophilic grain disease (FTDTAU-5)	5/7, 71%	0/23, 0%	4/20, 20%
Other 4R tauopathy (FTDTAU-6)	3/7, 43%	5/23, 22%	9/20, 45%
Tangle dominant disease (FTDTAU-9)	1/7, 14%	0/23, 0%	0/20, 0%
Other 3R/4R tauopathy (FTDTAU-10)	1/7, 14%	1/23, 4%	1/20, 5%

Abbreviations: aMCI, amnestic mild cognitive impairment; ADD, Alzheimer's disease dementia; F, female; FTD, frontotemporal degeneration; LATE-NC, limbic age-related TDP-43 encephalopathy neuropathologic change; M, male; *N*, sample size.

Notes: Average values are reported as mean ± standard deviation. A, B, C correspond to AD neuropathological change scores reflecting Thal amyloid phase (A), Braak neurofibrillary tangle stage (B), and Consortium to Establish a Registry for Alzheimer's Disease (CERAD) density of neuritic plaques (C). A/B/C scales are scored on a common semiquantitative 4-point scale from absent (0) to low (1), intermediate (2), and high (3).[25] TDP-43 staging followed an adapted version of the simplified staging system proposed by Nelson et al.:[3] 1 – TDP-43 in amygdala only; 2 – TDP-43 in hippocampus or entorhinal/inferior temporal cortex, but not frontal neocortex; 3 – TDP-43 in frontal neocortex and any of the other regions (see supporting information for more detailed information on TDP-43 assessment and individual staging). Scoring of Lewy body pathology follows consensus criteria from McKeith et al.:[47] 1 – brainstem predominant; 2 – limbic transitional, 3 – diffuse neocortical, 4 – amygdala predominant. FTDTDP and FTDTAU-X codes in parentheses refer to the respective pathologic designations in the Neuropathology Data Form of the National Alzheimer Coordinating Center (v10; https://www.alz.washington.edu/NONMEMBER/NP/npform10.pdf).

inferior temporal FDG-PET signal was lower in AD compared to LATE-NC (d = −0.91, $P = 0.044$; Figure 2). Accordingly, the IMT ratio was higher in LATE-NC compared to AD (d = −1.72, $P < 0.001$) and distinguished between the groups with an area under the curve (AUC) of 0.85 ($P = 0.007$). ROI values and IMT ratio of the AD+LATE-NC group did not differ significantly from the AD group ($P = 0.21$). However, the two HS cases in this group had IMT ratios at or above the average of the LATE-NC group, and their brain-wide hypometabolic pattern also showed a high correspondence to the LATE-NC pattern (Figure S4 in supporting information).

In vivo patient stratification based on autopsy-derived FDG-PET patterns

The automated pattern matching approach identified a subset of 25 clinically diagnosed AD dementia patients whose hypometabolic pattern was much more similar to the LATE-NC–typical pattern than to the AD pattern (i.e., $\Delta r \leq -0.28$). Not surprisingly, a much larger portion of the cohort ($N = 77$) was classified as having a relatively clean AD-typical FDG-PET pattern ($\Delta r > 0.28$), while others ($N = 78$) showed mixed regional hypometabolic features and could not be clearly matched to any of the two extremes ($-0.28 < \Delta r < 0.28$; Figure 3). Finally, there were also several patients that could not be assigned along the AD/LATE-NC pattern spectrum because they either lacked evidence of hypometabolism in any of the relevant areas ($N = 28$) or exhibited atypical regional features ($N = 34$) that were not consistent with any of the two patterns (Figure S5 in supporting information). These latter patient groups were omitted from further analyses in the current study.

Table 2 summarizes demographic, clinical, biomarker, and genetic characteristics of the two stratified patient groups. Patients with a LATE-NC–like FDG-PET pattern were on average almost 10 years older than AD-like cases (81.2 vs. 71.4 years, d = −1.28, $P < 0.001$). The patient groups did not differ in overall dementia severity as indicated by MMSE scores (d = −0.02; $P = 0.93$), but patients with a LATE-NC–like FDG-PET pattern were less impaired in memory (d = −0.56, $P = 0.017$) and especially in executive function (d = −0.81, $P < 0.001$) composite scores, and correspondingly showed a more memory-predominant cognitive deficit as indicated by the ΔMEM-EXEC cognitive profile variable (d = 0.53, $P = 0.023$). LATE-NC–like patients also showed a significantly slower longitudinal decline in all cognitive scores over follow-up (P's < 0.002; Figure S6 in supporting information).

Molecular CSF biomarkers showed significantly less abnormal $A\beta_{1\text{-}42}$ (d = −1.42, $P < 0.001$) and p-tau181 levels (d = 0.61, $P = 0.011$)

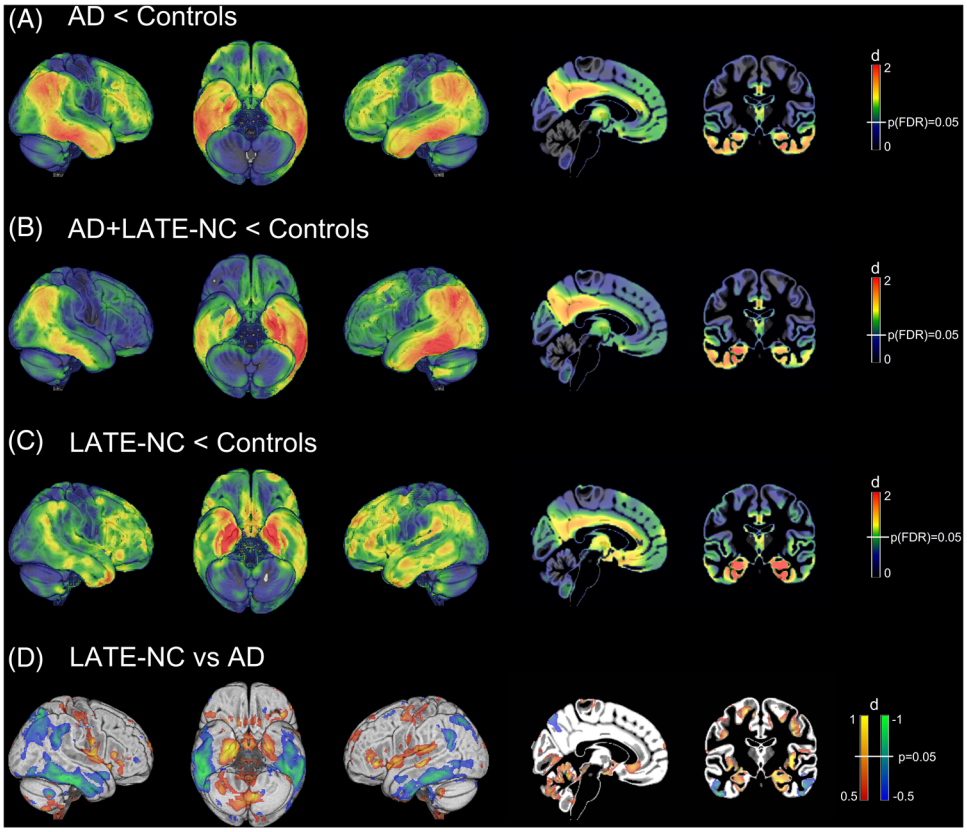

FIGURE 1 Pathology-specific fluorodeoxyglucose positron emission tomography (FDG-PET) patterns. Illustration of Alzheimer's disease (AD)–typical and limbic age-related TDP-43 encephalopathy neuropathologic change (LATE-NC)–typical hypometabolic patterns as estimated by voxel-wise comparisons of FDG-PET maps between the pathology-defined AD, AD+LATE-NC, and LATE-NC patient groups and the cognitively normal control group ($N = 179$). Statistical parametric maps of the respective group differences are expressed as Cohen's d effect size maps to reveal the brain-wide hypometabolic patterns. White vertical bars in the color scales on the right indicate the color of brain regions that meet the indicated statistical significance threshold. In the direct comparison between the LATE-NC and AD groups no voxels survived false discovery rate correction for the multiple voxel-wise testing. In this comparison, the blue-green color scale indicates more pronounced hypometabolism in AD and the red-yellow color scale indicates more pronounced hypometabolism in LATE-NC

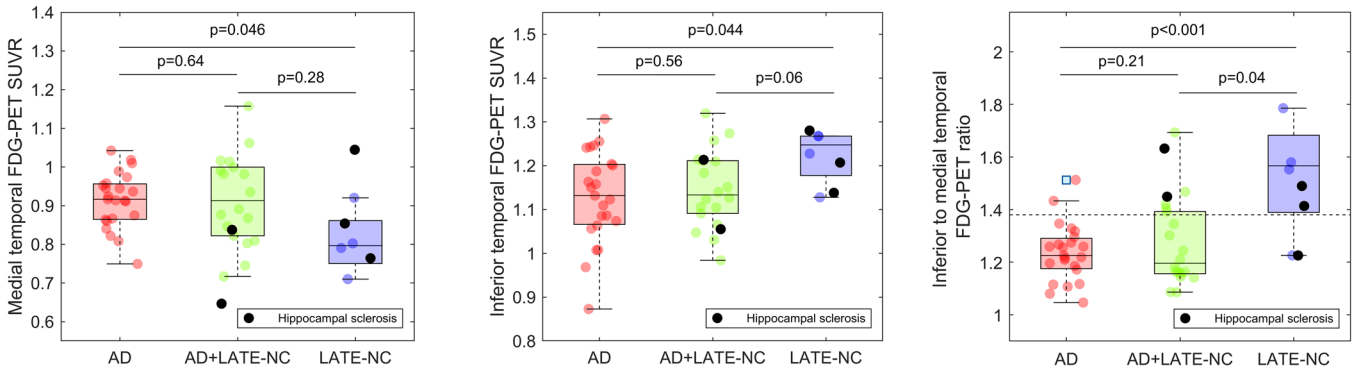

FIGURE 2 Metabolic differences between pathology defined limbic age-related TDP-43 encephalopathy neuropathologic change (LATE-NC), Alzheimer's disease (AD), and AD+LATE-NC patients in inferior and medial temporal regions of interest. Differences in fluorodeoxyglucose positron emission tomography (FDG-PET) standardized uptake value ratios (SUVR) between pathology-defined LATE-NC, AD, and AD+LATE-NC patients were assessed in medial temporal (left column) and inferior temporal (middle column) regions of interest, as well as using the inferior to medial temporal (IMT) ratio (right column). Reported *P*-values correspond to two-sample *t*-tests. The dotted line in the right column panel represents the Youden index-based optimal cut-off for the discrimination between LATE-NC and AD patients. Cases with hippocampal sclerosis are highlighted by black color (see Figures S4 and S8 in supporting information for visualizations of their brain-wide hypometabolic patterns)

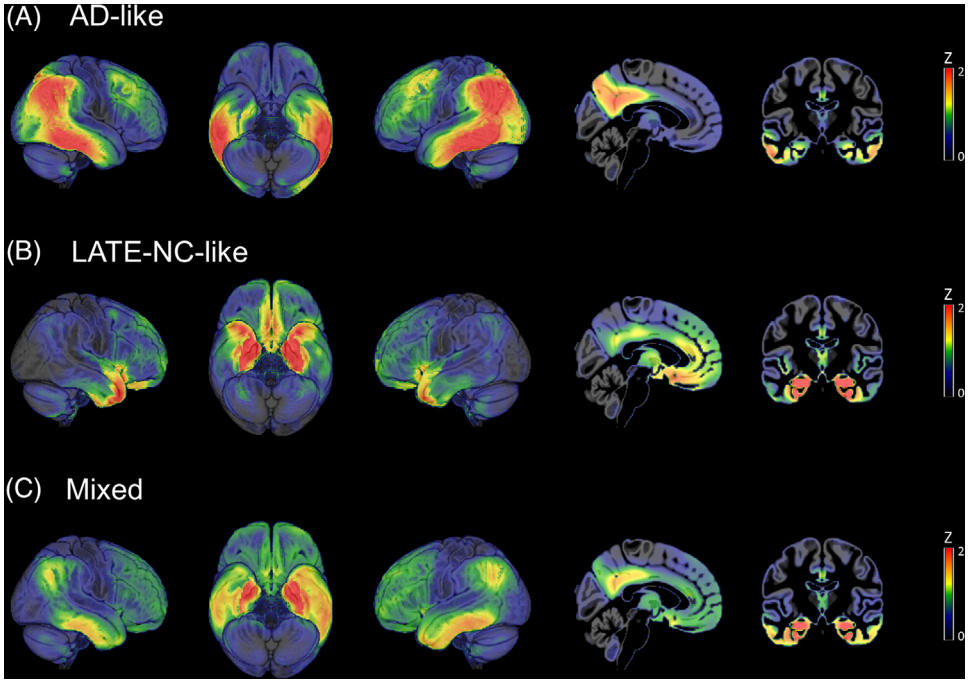

FIGURE 3 Fluorodeoxyglucose positron emission tomography (FDG-PET) patterns of the stratified Alzheimer's disease (AD)–like, limbic age-related TDP-43 encephalopathy neuropathologic change (LATE-NC)–like, and mixed patient groups in the in vivo cohort. Figure shows average Z-score maps of clinically diagnosed AD dementia patients from the in vivo cohort that were classified by the automated pattern matching algorithm as having clearly AD-like (A), clearly LATE-NC–like (B), or mixed (C) FDG-PET patterns of hypometabolism. Note that average Z-scores are equivalent to Glass' Δ effect size

TABLE 2 Characteristics of stratified patient groups in the in vivo cohort

	Total sample ($N = 242$)	LATE-NC–like ($N = 25$)	AD-like ($N = 77$)
Age (years)	74.9 ± 8.0	**81.2 ± 6.2**	**71.4 ± 8.1**
Sex (M/F)	143/99	15/10	41/36
Education (years)	15.3 ± 2.9	15.1 ± 3.1	15.6 ± 2.6
MMSE	23.2 ± 2.1	23.1 ± 2.0	23.0 ± 2.1
MEM	−0.89 ± 0.53	**−0.75 ± 0.46**	**−1.03 ± 0.53**
EXEC	−0.92 ± 0.93	**−0.54 ± 0.80**	**−1.24 ± 0.88**
Δ(MEM-EXEC)	0.03 ± 0.80	**−0.20 ± 0.79**	**0.21 ± 0.77**
CSF $A\beta_{42}$ (pg/ml)	704 ± 433	**1283 ± 822**	**625 ± 263**
CSF p-tau181 (pg/ml)	37 ± 16	**31 ± 16**	**41 ± 16**
APOE, 0/1/2 ε4 alleles, %pos	82/112/47, 66%	**13/12/0, 48%**	**25/36/16, 68%**
TMEM106B, 0/1/2 T alleles, % pos	36/105/69, 83%	*2/8/11, 91%*	*13/38/20, 82%*
GRN, 0/1/2 T alleles, % pos	104/80/26, 51%	8/8/5, 62%	31/32/8, 56%

Abbreviations: AD, Alzheimer's disease; *APOE*, apolipoprotein E; CSF, cerebrospinal fluid; EXEC, executive function composite score; F, female; LATE-NC, limbic age-related TDP-43 encephalopathy neuropathologic change; M, male; MEM, memory composite score; MMSE, Mini-Mental State Examination; *N*, sample size.

Notes: Significant differences (at $P < 0.05$) between LATE-NC–like and AD-like groups are printed in bold, differences with trend-level statistical significance ($P < 0.1$) are printed in italics.

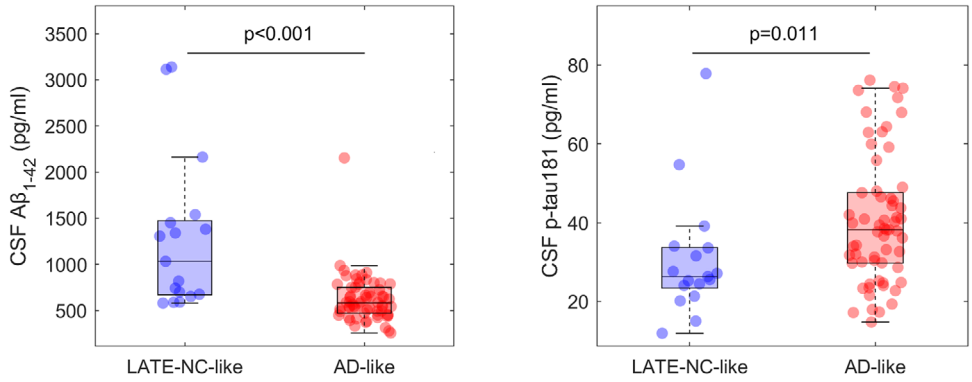

FIGURE 4 Amyloid beta (Aβ) and tau biomarker levels of limbic age-related TDP-43 encephalopathy neuropathologic change (LATE-NC)–like and Alzheimer's disease (AD)–like patients. Cerebrospinal fluid biomarker levels of A$\beta_{1\text{-}42}$ and phosphorylated tau (p-tau)181 among clinically diagnosed AD dementia patients showing a LATE-NC–like (blue) or an AD-like (red) hypometabolic pattern on fluorodeoxyglucose positron emission tomography (FDG-PET). Reported *P*-values correspond to a Mann-Whitney U test

in cases with a LATE-NC–like compared to a classical AD-like FDG-PET pattern (Figure 4). LATE-NC–like patients also had a significantly lower risk of carrying an *APOE* ε4 allele (odds ratio [OR] = 0.39; P = 0.014), and, by contrast, showed a trend toward higher allele load of the *TMEM106B* "T" risk allele (OR = 2.13; P = 0.057). Allele load of the *GRN* "T" risk allele was not significantly different between the stratified patient groups in this sample (OR = 1.44; P = 0.30).

In complementary analyses, pathologic pattern expression as a continuous variable (Δr) showed largely the same associations as for the dichotomous comparison of the two extremes (|Δr|>0.28; Figure S7 in supporting information). Moreover, the IMT ratio was highly correlated with the AD/LATE-NC pattern expression variable Δr (r = −0.83) and resulted in a similar patient stratification, though effect sizes of group differences were generally lower compared to the stratification based on pattern matching (Tables S3 and S4 in supporting information).

4 | DISCUSSION

On visual comparison, the distinct temporo-limbic FDG-PET pattern characterizing the LATE-NC cases in our study appears to be largely identical to the LATE-NC/HS-associated FDG-PET pattern reported in the previous study by Botha et al.[21] Accordingly, the IMT ratio capturing this pattern also distinguished the LATE-NC and AD groups with high accuracy (AUC = 0.85), which was almost identical to the accuracy reported for the distinction between HS (N = 6) and non-HS (N = 67) autopsy cases in a recent study by Buciuc et al. (AUC = 0.86).[20] However, in our study sample the distinct LATE-NC pattern was not solely driven by cases with HS (see Figure 2 and Figure S8 in supporting information). Interestingly, the FDG-PET pattern of the combined AD+LATE-NC cases did not markedly differ from the AD-typical pattern on a group level, although inter-individual variability was high and the patterns of the two HS cases in this group were indeed more similar to the LATE-NC pattern (Figure 2, Figure S4). This suggests that in the context of fully developed AD pathology (all but one individual had ADNC = 3), LATE-NC may have a more variable effect on the neurodegeneration phenotype.

Using an automated pattern matching approach, we identified a subset of 10% of clinically diagnosed AD dementia patients whose FDG-PET pattern more closely resembled the autopsy-derived LATE-NC pattern than a typical AD pattern. This proportion also roughly corresponds to the proportion of "pure" LATE-NC cases (i.e., not concurrently fulfilling pathologic criteria for AD) in autopsy studies of clinically diagnosed AD dementia patients.[3,7,10] However, it is important to note that the relative proportions of the stratified patient groups in the present study also strongly depend on the specific methodology used for classifying the FDG-PET scans, and in particular on the rather arbitrary cutoff used for separating the upper and lower parts of the Δr distribution into relatively clean AD-like and LATE-NC–like patterns (Figure S2). Similar to our automated classification approach based on spatial correspondence, a commonly used approach for aiding differential dementia diagnosis in the clinical setting is to visually assess the correspondence of an individual patient's FDG-PET pattern with a (predefined) set of known dementia-specific FDG-PET patterns.[38] Pending further validation in larger autopsy-confirmed patient samples, the reported temporo-limbic FDG-PET pattern could be used in such expert ratings as being suggestive of LATE-NC in the differential diagnosis of amnestic dementia.

Because autopsy information is not yet available for the in vivo cohort, the actual underlying pathologies of the patients with a LATE-NC–like FDG-PET pattern remain unknown. However, analysis of pathologically well-validated molecular AD biomarkers[34] demonstrated that these individuals indeed had significantly lower levels of AD pathology, indicating that other, non-AD pathologic factors account for their cognitive deficits. Previous research has suggested to pre-screen older amnestic patients by a negative amyloid or tau biomarker finding, which would exclude AD as the principal pathologic substrate for the cognitive deficits.[21,39–41] Correspondingly, Botha et al.[21] could demonstrate that older amnestic patients with a negative tau-PET scan showed a very similar temporo-limbic FDG-PET

pattern compared to patients with autopsy-confirmed LATE-NC and HS. However, in our study many patients with a clear LATE-NC–like FDG-PET pattern had CSF p-tau181 levels above commonly used positivity thresholds (ranging between 19 and 27 pg/ml;[34] see Figure 4). Recent studies have shown that CSF p-tau181 increases are more closely related to early, presymptomatic AD pathology, whereas elevated tau-PET signal is more closely linked with progressive neurodegeneration and cognitive deterioration.[42,43] Hence, suprathreshold CSF p-tau181 levels may not necessarily indicate neurofibrillary tangle pathology levels that would be sufficient to account for a clinical dementia syndrome. On the other hand, negative tau (or amyloid) biomarker findings in older amnestic patients are unlikely to be specific for LATE-NC because there are several different impactful pathologic conditions (often present in combination) associated with advanced age.[1,2,41,44]

In addition to lower AD biomarker levels, patients with a LATE-NC–like FDG-PET pattern showed several clinical and genetic features that were previously linked to LATE-NC in pathologic studies, particularly older age, a more memory-predominant cognitive profile with an overall slower disease course, as well as enrichment for the *TMEM106B* risk allele.[3,11,14] In line with the intermediate *APOE ε4* prevalence reported for autopsy-confirmed LATE-NC cases,[15,16] patients with a LATE-NC–like FDG-PET pattern also showed a significantly lower *APOE ε4* allele load compared to typical AD-like patients, albeit still enriched compared to a population level of ≈25%. In summary, these data suggest that amnestic dementia patients with a LATE-NC–like FDG-PET pattern show several clinical, biomarker, and genetic features consistent with underlying LATE-NC. However, one cannot exclude that other age-related pathologies that preferentially target the medial temporal lobe, such as primary age-related tauopathy, argyrophilic grain disease, or limbic-predominant AD, may also be present in subsets of these patients, especially given that these pathologies often overlap with LATE-NC.[6,12,44] Nevertheless, we have conducted several sensitivity analyses that corroborate the specificity of the reported temporolimbic FDG-PET pattern for LATE-NC as opposed to advanced age or other commonly comorbid age-related pathologies (see supporting information and Figures S9 to S12 for extended analyses and discussion).

One principal limitation of the present study is the relatively small sample size of the autopsy-confirmed LATE-NC cases used to estimate the LATE-NC–specific FDG-PET pattern that is subsequently used in the pattern matching approach. However, the estimated pattern showed a remarkable spatial resemblance to the LATE-NC/HS-associated FDG-PET pattern reported in a previous autopsy study with similar sample size,[21] and we could further confirm this pattern in two additional autopsy cases with HS that were excluded from initial pattern estimation due to comorbid AD pathology (Figure S4). Moreover, a comparison between in vivo stratification approaches indicated that pattern matching to the autopsy-derived FDG-PET patterns (dependent on our study sample) yielded a comparable or slightly higher enrichment for LATE-NC–characteristic features compared to stratification based on the "a priori" IMT ratio. Future studies are warranted that will assess the utility of this pattern-based classification approach for identifying patients with a LATE-NC–like neurodegeneration pattern at a pre-dementia disease stage and to study their disease evolution over clinical follow-up.[45,46]

ACKNOWLEDGMENTS

Michel J. Grothe is supported by the "Miguel Servet" program (CP19/00031) and a research grant (PI20/00613) of the Instituto de Salud Carlos III-Fondo Europeo de Desarrollo Regional (ISCIII-FEDER). Jesús Silva-Rodríguez is supported by the ISCIII-FEDER "Sara Borrell" program (CD21/00067). Kwangsik Nho receives support from NIH grant R01 LM013463. Andrew J. Saykin receives support from NIH grants P30 AG010133, P30 AG072976, R01 AG019771, R01 AG057739, U01 AG024904, R01 LM013463, R01 AG068193, T32 AG071444, U01 AG068057, and U01 AG072177. PN receives support from NIH grants R01 AG057187, P30 AG072946, and RF1 NS118584. Michael Schöll is supported by the Knut and Alice Wallenberg Foundation (Wallenberg Centre for Molecular and Translational Medicine; KAW 2014.0363), the Swedish Research Council (#2017-02869), the Swedish state under the agreement between the Swedish government and the County Councils, the ALF-agreement (#ALFGBG-813971), and the Swedish Alzheimer Foundation (#AF-740191). Data used in the preparation of this article were obtained from the ADNI database (http://adni.loni.usc.edu/). The ADNI was launched in 2003 as a public–private partnership, led by Principal Investigator Michael W. Weiner, MD. The primary goal of ADNI has been to test whether serial MRI, PET, other biological markers, and clinical and neuropsychological assessment can be combined to measure the progression of MCI and early AD. A fuller description of ADNI and up-to-date information is available at www.adni-info.org. ADNI is funded by grants from the NIH (U01 AG024904), Department of Defense (award number W81XWH-12-2-0012), National Institute on Aging, the National Institute of Biomedical Imaging and Bioengineering, and through generous contributions from the following: AbbVie; Alzheimer's Association; Alzheimer's Drug Discovery Foundation; Araclon Biotech; BioClinica, Inc.; Biogen; Bristol-Myers Squibb Company; CereSpir, Inc.; Cogstate; Eisai Inc.; Elan Pharmaceuticals, Inc.; Eli Lilly and Company; EuroImmun; F. Hoffmann-La Roche Ltd and its affiliated company Genentech, Inc.; Fujirebio; GE Healthcare; IXICO Ltd.; Janssen Alzheimer Immunotherapy Research & Development, LLC; Johnson & Johnson Pharmaceutical Research & Development LLC; Lumosity; Lundbeck; Merck & Co., Inc.; Meso Scale Diagnostics, LLC; NeuroRx Research; Neurotrack Technologies; Novartis Pharmaceuticals Corporation; Pfizer Inc.; Piramal Imaging; Servier; Takeda Pharmaceutical Company; and Transition Therapeutics. The Canadian Institutes of Health Research is providing funds to support ADNI clinical sites in Canada. Private sector contributions are facilitated by the Foundation for the National Institutes of Health (www.fnih.org). The grantee organization is the Northern California Institute for Research and Education, and the study is coordinated by the Alzheimer's Therapeutic Research Institute at the University of Southern California. ADNI data are disseminated by the Laboratory for Neuro Imaging at the University of Southern California.

Open access funding enabled and organized by Projekt DEAL.

CONFLICTS OF INTEREST

J.S.R. is an advisor and shareholder of Qubiotech Health Intelligence SL. A.J.S. has received support from Avid Radiopharmaceuticals, a subsidiary of Eli Lilly (in kind contribution of PET tracer precursor); Bayer Oncology (Scientific Advisory Board); Siemens Medical Solutions USA, Inc. (Dementia Advisory Board); Springer-Nature Publishing (Editorial Office Support as Editor-in-Chief, *Brain Imaging and Behavior*). S.J.T. participated in scientific advisory boards of Roche Pharma AG, Biogen, GRIFOLS, EISAI, and MSD, and received lecture fees from Roche and MSD. The other authors report no competing interests. Author disclosures are available in the supporting information.

REFERENCES

1. Mehta RI, Schneider JA. What is 'Alzheimer's disease'? The neuropathological heterogeneity of clinically defined Alzheimer's dementia. *Curr Opin Neurol*. 2021;34:237-245.
2. Serrano-Pozo A, Qian J, Monsell SE, et al. Mild to moderate Alzheimer dementia with insufficient neuropathological changes. *Ann Neurol*. 2014;75:597-601.
3. Nelson PT, Dickson DW, Trojanowski JQ, et al. Limbic-predominant age-related TDP-43 encephalopathy (LATE): consensus working group report. *Brain*. 2019;142:1503-1527.
4. Brenowitz WD, Monsell SE, Schmitt FA, Kukull WA, Nelson PT. Hippocampal sclerosis of aging is a key Alzheimer's disease mimic: clinical-pathologic correlations and comparisons with both alzheimer's disease and non-tauopathic frontotemporal lobar degeneration. *J Alzheimers Dis*. 2014;39:691-702.
5. Josephs KA, Whitwell JL, Weigand SD, et al. TDP-43 is a key player in the clinical features associated with Alzheimer's disease. *Acta Neuropathol*. 2014;127:811-824.
6. Josephs KA, Whitwell JL, Tosakulwong N, et al. TAR DNA-binding protein 43 and pathological subtype of Alzheimer's disease impact clinical features. *Ann Neurol*. 2015;78:697-709.
7. James BD, Wilson RS, Boyle PA, Trojanowski JQ, Bennett DA, Schneider JA. TDP-43 stage, mixed pathologies, and clinical Alzheimer's-type dementia. *Brain*. 2016;139:2983-2993.
8. Nag S, Yu L, Capuano AW, et al. Hippocampal sclerosis and TDP-43 pathology in aging and Alzheimer disease. *Ann neurol*. 2015;77:942-952.
9. Nag S, Yu L, Wilson RS, Chen EY, Bennett DA, Schneider JA. TDP-43 pathology and memory impairment in elders without pathologic diagnoses of AD or FTLD. *Neurology*. 2017;88:653-660.
10. Nelson PT. LATE neuropathologic changes with little or no Alzheimer disease is common and is associated with cognitive impairment but not frontotemporal dementia. *J Neuropathol Exp Neurol*. 2021;80:649-651.
11. Kapasi A, Yu L, Boyle PA, Barnes LL, Bennett DA, Schneider JA. Limbic-predominant age-related TDP-43 encephalopathy, ADNC pathology, and cognitive decline in aging. *Neurology*. 2020;95:e1951-e62.
12. Murray ME, Cannon A, Graff-Radford NR, et al. Differential clinicopathologic and genetic features of late-onset amnestic dementias. *Acta neuropathol*. 2014;128:411-421.
13. Nelson PT, Wang WX, Partch AB, et al. Reassessment of risk genotypes (GRN, TMEM106B, and ABCC9 variants) associated with hippocampal sclerosis of aging pathology. *J Neuropathol Exp Neurol*. . 2015;74:75-84.
14. Hokkanen SRK, Kero M, Kaivola K, et al. Putative risk alleles for LATE-NC with hippocampal sclerosis in population-representative autopsy cohorts. *Brain pathol. (Zurich, Switzerland)*. 2020;30:364-372.
15. Wennberg AM, Tosakulwong N, Lesnick TG, et al. Association of apolipoprotein e epsilon4 with transactive response DNA-binding protein 43. *JAMA neurol*. 2018;75:1347-54.
16. Yang HS, Yu L, White CC, et al. Evaluation of TDP-43 proteinopathy and hippocampal sclerosis in relation to APOE ε4 haplotype status: a community-based cohort study. *Lancet Neurol*. 2018;17:773-781.
17. Bejanin A, Murray ME, Martin P, et al. Antemortem volume loss mirrors TDP-43 staging in older adults with non-frontotemporal lobar degeneration. *Brain*. 2019;142:3621-3635.
18. Woodworth DC, Nguyen HL, Khan Z, Kawas CH, Corrada MM, Sajjadi SA. Utility of MRI in the identification of hippocampal sclerosis of aging. *Alzheimers Dement*. 2021;17:847-855.
19. de Flores R, Wisse LEM, Das SR, et al. Contribution of mixed pathology to medial temporal lobe atrophy in Alzheimer's disease. Alzheimer's & dementia : the journal of the Alzheimer's *Association*. 2020;16:843-852.
20. Buciuc M, Botha H, Murray ME, et al. Utility of FDG-PET in diagnosis of Alzheimer-related TDP-43 proteinopathy. *Neurology*. 2020;95:e23-e34.
21. Botha H, Mantyh WG, Murray ME, et al. FDG-PET in tau-negative amnestic dementia resembles that of autopsy-proven hippocampal sclerosis. *Brain*. 2018;141:1201-1217.
22. Johnson SC, Christian BT, Okonkwo OC, et al. Amyloid burden and neural function in people at risk for Alzheimer's Disease. *Neurobiol Aging*. 2014;35:576-584.
23. Levin F, Ferreira D, Lange C, et al. Data-driven FDG-PET subtypes of Alzheimer's disease-related neurodegeneration. *Alzheimers Res Ther*. 2021;13:49.
24. Franklin EE, Perrin RJ, Vincent B, Baxter M, Morris JC, Cairns NJ. Brain collection, standardized neuropathologic assessment, and comorbidity in Alzheimer's Disease Neuroimaging Initiative 2 participants. *Alzheimers Dement*. 2015;11:815-822.
25. Montine TJ, Phelps CH, Beach TG, et al. National Institute on Aging-Alzheimer's Association guidelines for the neuropathologic assessment of Alzheimer's disease: a practical approach. *Acta Neuropathol*. 2012;123:1-11.
26. Katsumata Y, Fardo DW, Kukull WA, Nelson PT. Dichotomous scoring of TDP-43 proteinopathy from specific brain regions in 27 academic research centers: associations with Alzheimer's disease and cerebrovascular disease pathologies. *Acta Neuropathol Commun*. 2018;6:142.
27. Lange C, Suppa P, Frings L, Brenner W, Spies L, Buchert R. Optimization of Statistical Single Subject Analysis of Brain FDG PET for the Prognosis of Mild Cognitive Impairment-to-Alzheimer's Disease Conversion. *J Alzheimers Dis*. 2016;49:945-959.
28. Grothe MJ, Teipel SJ. Spatial patterns of atrophy, hypometabolism, and amyloid deposition in Alzheimer's disease correspond to dissociable functional brain networks. *Hum Brain Mapp*. 2016;37:35-53.
29. Lakens D. Calculating and reporting effect sizes to facilitate cumulative science: a practical primer for t-tests and ANOVAs. *Front Psychol*. 2013;4:863.
30. Grothe MJ, Sepulcre J, Gonzalez-Escamilla G, et al. Molecular properties underlying regional vulnerability to Alzheimer's disease pathology. *Brain*. 2018;141:2755-2771.
31. Whitwell JL, Graff-Radford J, Tosakulwong N, et al. Imaging correlations of tau, amyloid, metabolism, and atrophy in typical and atypical Alzheimer's disease. *Alzheimers Demen*. 2018;14:1005-1014.
32. Crane PK, Carle A, Gibbons LE, et al. Development and assessment of a composite score for memory in the Alzheimer's Disease Neuroimaging Initiative (ADNI). *Brain Imaging Behav*. 2012;6:502-516.
33. Gibbons LE, Carle AC, Mackin RS, et al. A composite score for executive functioning, validated in Alzheimer's Disease Neuroimaging Initiative (ADNI) participants with baseline mild cognitive impairment. *Brain Imaging Behav*. 2012;6:517-527.
34. Grothe MJ, Moscoso A, Ashton NJ, et al. *Associations of Fully Automated CSF and Novel Plasma Biomarkers With Alzheimer Disease Neuropathology at Autopsy*. Neurology. 2021.

35. Saykin AJ, Shen L, Yao X, et al. Genetic studies of quantitative MCI and AD phenotypes in ADNI: progress, opportunities, and plans. *Alzheimers Deme*. 2015;11:792-814.
36. Nho K, Saykin AJ, Nelson PT. Hippocampal sclerosis of aging, a common alzheimer's disease 'mimic': risk genotypes are associated with brain atrophy outside the temporal lobe. *J Alzheimers Dis*. 2016;52:373-83.
37. Armstrong RA. When to use the Bonferroni correction. *Ophthalmic Physiol Opt*. 2014;34:502-508.
38. Nestor PJ, Altomare D, Festari C, et al. Clinical utility of FDG-PET for the differential diagnosis among the main forms of dementia. *Eur J Nucl Med Mol Imaging*.. 2018;45:1509-1525.
39. Stage EC, Jr., Svaldi D, Phillips M, et al. Neurodegenerative changes in early- and late-onset cognitive impairment with and without brain amyloidosis. *Alzheimers Res Ther*. 2020;12:93.
40. Chételat G, Ossenkoppele R, Villemagne VL, et al. Atrophy, hypometabolism and clinical trajectories in patients with amyloid-negative Alzheimer's disease. *Brain*. 2016;139:2528-2539.
41. McCollum LE, Das SR, Xie L, et al. Oh brother, where art tau? Amyloid, neurodegeneration, and cognitive decline without elevated tau. *Neuroimage Clin*. 2021;31:102717.
42. Ossenkoppele R, Reimand J, Smith R, et al. Tau PET correlates with different Alzheimer's disease-related features compared to CSF and plasma p-tau biomarkers. *EMBO Mol Med*. 2021:e14398.
43. Moscoso A, Grothe MJ, Ashton NJ, et al. Time course of phosphorylated-tau181 in blood across the Alzheimer's disease spectrum. *Brain*. 2020.
44. Jicha GA, Nelson PT. Hippocampal sclerosis, argyrophilic grain disease, and primary age-related tauopathy. *Continuum (Minneapolis, Minn)*. 2019;25:208-33.
45. Tondo G, Carli G, Santangelo R, et al. Biomarker-based stability in limbic-predominant amnestic mild cognitive impairment. *Eur J Neurol*.. 2021;28:1123-1133.
46. Cerami C, Della Rosa PA, Magnani G, et al. Brain metabolic maps in Mild Cognitive Impairment predict heterogeneity of progression to dementia. *Neuroimage Clin*. 2015;7:187-194.
47. McKeith IG, Dickson DW, Lowe J, et al. Diagnosis and management of dementia with Lewy bodies: third report of the DLB Consortium. *Neurology*. 2005;65:1863-1872.

SUPPORTING INFORMATION

Additional supporting information can be found online in the Supporting Information section at the end of this article.

How to cite this article: Grothe M, Moscoso A, Silva-Rodríguez J, et al. Differential diagnosis of amnestic dementia patients based on an FDG-PET signature of autopsy-confirmed LATE-NC. *Alzheimer's Dement*. 2022;1-11. https://doi.org/10.1002/alz.12763